Materials Characterization 142 (2018) 68–76

Contents lists available at ScienceDirect

Materials Characterization

journal homepage: www.elsevier.com/locate/matchar

Secondary recrystallization behavior in strip-cast grain-oriented silicon steel processed by isothermal secondary annealing

X. Lu[a], F. Fang[a], Y.X. Zhang[a,*], Y. Wang[a], G. Yuan[a], R.D.K. Misra[b], W.N. Zhang[a], G.D. Wang[a]

[a] State Key Laboratory of Rolling and Automation, Northeastern University, Shenyang 110819, China
[b] Laboratory for Excellence in Advanced Steel Research, Department of Metallurgical, Materials and Biomedical Engineering, University of Texas at El Paso, El Paso, TX 79912, USA

ARTICLE INFO

Keywords:
Grain-oriented silicon steel
Secondary recrystallization
Strip-cast
Goss texture

ABSTRACT

The primary annealed sheets of strip-cast grain-oriented silicon steel were isothermally secondary annealed for 15 min under 100% H_2 atmosphere. The microstructure and crystallographic orientation at different annealing temperatures were characterized and the secondary recrystallization behavior was elucidated. It was observed that relatively complete abnormal grain growth occurred at 1025 °C. Incomplete abnormal grain growth developed when the temperature was lower than 1025 °C, and normal grain growth occurred when the temperature was higher than 1025 °C. During the abnormal grain growth, both of the Goss and {110}⟨227⟩ grains developed because of the rapid decrease of the inhibiting force and the limited annealing time. Considering the high energy boundary (HE), coincidence site lattice boundary (CSL) and solid-state wetting (SSW) models for abnormal grain growth, the first one explained the development of the Goss and {110}⟨227⟩ grains. Another result was that several matrix grain colonies were observed in the interior or at the boundaries of secondary grains after abnormal grain growth. The grains at the periphery of these colonies showed a large fraction of high energy boundaries (20–45° misorientation) with the surrounding secondary grain and similar grain size with the unconsumed matrix grains. Therefore, these colonies were expected to be consumed by prolonging the annealing time and thus the limited annealing time was responsible for their occurrence. A possible explanation for the dominated high energy boundaries instead of low energy boundaries at the periphery of these colonies was proposed. All of these behaviors promoted the understanding of abnormal grain growth.

1. Introduction

Grain-oriented silicon steels are characterized by a sharp {110}⟨001⟩ (Goss) texture, and are primarily used as transformer core materials [1]. The production route in the industry of these steels uses thick casting slab, which is developed from the method proposed by Goss in 1934 [2]. Recently, a novel strip casting method was reported to produce grain-oriented silicon steel [3]. This method uses ~2–5 mm as-cast strip instead of thick casting slab [4,5]. It is considered the process of the future because of its high efficiency and low cost. In both conventional route and strip casting route, the sharp Goss texture is the result of a long-term batch secondary annealing, also known as high-temperature annealing. Generally, the steels are heated to 1200 °C at a slow heating rate of 15–20 °C/h and then kept at this temperature for 30–40 h. This is ineffective and high-cost. Therefore, a short isothermal secondary annealing was proposed in recent years.

During the stage, Gunther and co-workers [6] proposed an isothermal annealing process for grain-oriented silicon steel which contained primary annealing, high-temperature nitriding and secondary annealing. All of these processes were completed in ~8 min. They carried out some basic experiment and concluded the nitriding was a decisive step. Later, Stoyka et al. [7] isothermally annealed the cold rolled grain-oriented silicon steel at different temperatures and stated the optimal magnetic properties were obtained at 1015 °C for 10 min. They found the magnetic properties after isothermal annealing were inferior to batch annealing and attributed this to the retained inhibitors. More recently, Jiao et al. [8] reported the isothermal secondary annealing can be used in the low slab-reheating temperature route, and found that secondary grains with {110} orientation other than Goss orientation were developed. This significantly decreased the magnetic induction. However, this was not emphasized in Stoyka's work. All of these published studies concentrated on the relationship between the annealing parameters and final magnetic properties. The detailed secondary recrystallization behavior continues to be unclear. Specifically, the development of {110} grains other than Goss grains needs to be confirmed and their formation mechanism should be

* Corresponding author at: No.11, Lane No.3, Wenhua Road, Heping District, Shenyang 110819, China.
E-mail address: neuzhangyuanxiang@126.com (Y.X. Zhang).

https://doi.org/10.1016/j.matchar.2018.05.029
Received 21 January 2018; Received in revised form 8 May 2018; Accepted 16 May 2018
Available online 18 May 2018

elucidated. In addition, the annealing time of the isothermal secondary annealing was much shorter than the batch secondary annealing, which may induce different microstructure. All of these behaviors are not reported to the best of our understanding, and comparisons between these behaviors and batch secondary recrystallization behaviors have not been made.

In the current study, the microstructure and crystallographic orientation of strip-cast grain-oriented silicon steel after isothermal secondary annealing were characterized by electron backscattered diffraction (EBSD) and transmission electron microscopy (TEM). Based on these results, the secondary behavior was clarified and compared with the batch secondary annealing. This study contributed to the understanding of abnormal grain growth.

2. Experimental

The material used in this study was grain-oriented 4.5%Si steel containing: 4.48 Si, 0.003 C, 0.225 Mn, 0.01 Al, 0.026 S, 0.008 N, 0.035 Nb (in mass percent). The raw materials were melted in a vacuum induction furnace and then poured into a strip caster as described previously [9]. The width and thickness of the as-cast strip were 110 mm and ~2.5 mm, respectively. The as-cast strip was warm rolled to 0.75 mm at 380–400 °C (referred to as 1st rolling). The reduction ratio of the first three passes was controlled to be 3%–5%. After that, the reduction ratio of per pass gradually increased from 8% to 15%. After 1st rolling, the sheet was intermediate annealed at 1050 °C for 5 min (under 100% N_2) and then rolled to 0.23 mm at a relatively low temperature of 250–300 °C (referred to as 2nd rolling). The reduction ratio was similar to 1st rolling. The 2nd rolled sheet was primarily annealed at 750 °C for 8 min (under 100% N_2). The primary annealed sheet was then isothermally annealed at 950 °C, 1000 °C, 1025 °C and 1100 °C for 15 min under 100% H_2. Also, a sample was annealed at 1000 °C for 4 h to make a comparison. The annealing treatment was carried out in an atmospheric furnace made by our group. Fig. 1 shows the schematic diagram of the furnace. The sample was initially placed in the preparation region which was separated from the heating furnace by a door. After the furnace reaching the preset temperature, the door was opened and the sample was pushed into the furnace by a pushing rod. When the annealing was finished, the sample was pulled out and cooled under H_2 atmosphere.

The microstructure and crystallographic orientation of the subsurface containing rolling direction (RD) and transverse direction (TD) were examined by EBSD method. The sample was electropolished using a 7:1 volume ratio of perchloric acid and methanol mixture. The polishing was performed at 20 V and room temperature. EBSD data acquisition was carried out using an Oxford Instruments attached to scanning electron microscope (SEM, Zeiss Ultra 55). The step size was chosen from 1.5–5 μm. After the acquisition, the data were post-processed by HKL Channel 5 software. During post-processing, it was found that some incorrect points occurred especially in the interior of secondary grains which were attributed to the pseudosymmetry of the crystal. Using the boundary highlighting mode, the misorientation between these incorrect points and the surrounding grains was found to be approximately 30°or 60° around ⟨111⟩ direction. This orientation relationship was considered during post-processing and the incorrect points were cleaned up. The second-phase particles after secondary annealing were observed and identified by TEM (Tecnai G20) with energy dispersive spectroscopy (EDS, EDAX) system. The specimens for the TEM test were twin-jet electropolished at 25 V and − 25 °C using Tenupol 5 machine. The polishing solution was 7:1 volume ratio of perchloric acid and methanol mixture. The magnetic induction B_8 and core losses $P_{10/1000}$ of the samples were measured by using a single sheet tester. The dimensions of the sample were 30 mm in the TD and 100 mm in the RD.

3. Results

In the current silicon steel, the high silicon content increased the hardness and resulted in brittle Fe-Si ordered phases. This led to poor workability so the rolling strategy of the conventional 3.0%Si steel cannot be used. Thus, a warm rolling method characterized by increasing pass reduction ratio and decreasing rolling temperature was adopted. At the initial stage of 1st rolling, the small pass reduction ratio satisfied the workability of the ordered phases and the deformation temperature improved the mobility of the super dislocations in it. Therefore, the steel can be successfully deformed. With the progress of rolling, the order of the steel was destroyed because of the formation of anti-phase boundaries [10]. The plasticity of the steel was gradually improved, and thus the pass reduction ratio increased. After intermediate annealing, although new ordered phases formed during cooling, complete recrystallization occurred. This resulted in a good plasticity, and thus the rolling temperature of 2nd rolling was decreased. Another thing to be mentioned was that the warm rolling also strengthened the softening effect by recovery. This offset work hardening effect to some extent and reduced the hardness of the steel. Based on this rolling strategy, the high silicon steel was successfully rolled to 0.23 mm. Fig. 2 shows the final sheet which is pickled. Only some 0.5–1.5 mm edge cracks can be observed (Fig. 2b). This suggested the rolling strategy was suitable.

Fig. 3 shows the grain unique color map and corresponding ODF section of the subsurface (1/4 thickness) of the primary annealed sheet. The primary annealed sheet was characterized by completely equiaxed grains with an average size of ~8–9 μm (Fig. 3a). The texture consisted of typical γ-fiber (⟨111⟩//ND) and {001}⟨100⟩ (Cube) texture (Fig. 3b). It should be mentioned that the surface texture of the same sample exhibited dominated γ-fiber (⟨111⟩//ND) but quite a weak Cube texture, as mentioned in our previous study [11]. This implied a texture gradient along the thickness. Although Goss component was not observed in the ODF section, several Goss grains were observed (the green grains in Fig. 3a). The magnetic induction B_8 after primary annealing was 1.482 T. One aspect to be noted was that the high silicon content in the current study decreased the supersaturated magnetic induction (B_s). The B_s was 2.03 T for 3.0%Si steel and 1.90 T for 4.5%Si steel. Therefore, the grains showing 1.482 T (1.482/1.90 = 0.78) in the

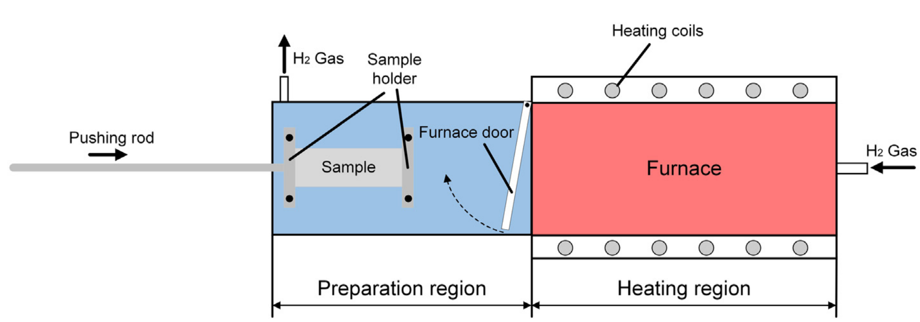

Fig. 1. The schematic diagram of the annealing furnace.